STATUS OF NSLS-II BOOSTER

S.Gurov, A.Erokhin, S.Karnaev, V.Kiselev, E.Levichev, A.Polyansky, A.Semenov, S.Shiyankov, S.Sinyatkin, V.Smaluk, BINP SB RAS, Novosibirsk, Russia; T.Shaftan, H. Hseuh, Photon Sciences, BNL, Upton, NY, 11973, U.S.A

Abstract

The National Synchrotron Light Source II is a third generation light source under construction at Brookhaven National Laboratory. The project includes a highly optimized 3 GeV electron storage ring, linac pre-injector and full-energy injector-synchrotron. Budker Institute of Nuclear Physics has built the booster for NSLS-II. The booster should accelerate the electron beam continuously and reliably from a minimum 170-MeV injection energy to a maximum energy of 3.15 GeV and an average beam current of 20 mA. The booster should be capable of multi-bunch and single bunch operation. The main achieved parameters and features of the booster systems are discussed in this paper.

INTRODUCTION

The injector system includes a 200-MeV linac and the booster with energy up to 3GeV. The preliminary design was by BNL [1]. The tender on the design, production and commissioning of NSLS-II booster was started in January 2010. Budker Institute of Nuclear Physics won this tender in May 2010. The booster was designed [2], produced, delivered, assembled and tested.

BOOSTER MECHANICAL DESIGN

The design of the booster began in June 2010. About thirty BINP designers participated in this work. Most work, including the complete 3D model of the booster, was made in the 3D design software Inventor. The development and design of the basic units of the booster were completed in 2011. After transfer of the drawings to the workshops, 3 leading designers were providing support to the project. The final set of 2D drawings and 3D models of the booster were transferred to BNL in December 2012.

MAGNETIC SYSTEM

All booster magnets were made at BINP. The BINP workshop has designed and produced all dies for magnet laminations with the accuracy up to 5 μm on the critical surfaces.

The end chamfers of the dipole and quadrupole prototypes were milled on the magnet yoke in two iterations. First, the magnets were measured without the end chamfers. Then the end chamfers were milled at ¾ of the calculated depth. After this, the design of the final end chamfers was corrected taking into account the magnetic measurement results. The BF and BD dipoles have complicated end chamfers. After magnetic calculation, the 3D model of the dipole yokes was transferred to a designer. The designer processed the 3D model and sent it to the workshop for a milling machine and a coordinate-measurement machine to check the produced end chamfers. As a result, the prototypes meet the specifications after two iterations.

The BF and BD dipole magnets were measured with the Hall sensors. The measurement method and results are described in the papers [3, 4]. The relative measured accuracy of the basic integral parameters of the dipole magnets at nominal fields is the following: the field integral is measured with accuracy better than 7×10^{-5}, the field gradient integral is measured with accuracy better than 5×10^{-4}, the sextupole component of the field integral is measured with accuracy better than 8×10^{-3}. The measurement results are summarized in Tables 1 and 2. The produced magnets meet the specifications.

Table 1: The Relative Accuracy (rms) for BD Dipole

Current, A	49.8	74.6	123.8	368.2	742.0
Calculated energy, GeV	0.20	0.30	0.50	1.50	3.00
Effective magnetic length, %	0.01	0.01	0.01	0.01	0.01
Field Integral, %	0.07	0.07	0.07	0.06	0.00
dK1/K1, %	0.19	0.19	0.18	0.17	0.16
dK2/K2, %	1.42	1.33	1.03	0.66	0.55

Table 2: The Relative Accuracy (rms) for BF Dipole

Current, A	58.3	87.1	145.4	432.1	863.7
Calculated energy, GeV	0.21	0.31	0.51	1.50	3.00
Effective magnetic length, %	0.02	0.02	0.02	0.02	0.02
Field Integral, %	0.10	0.07	0.04	0.03	0.00
dK1/K1, %	0.09	0.07	0.04	0.04	0.04
dK2/K2, %	1.55	1.77	1.40	0.47	0.48

The pulsed magnetic measurements of the dipoles were performed to estimate the influence of the vacuum chamber on the magnetic fields in the dipoles. The method of measurements and magnetic measurement results are presented in the report at this conference [5].

POWER SUPPLIES

The Booster magnetic system requires 59 Power Supplies with a total peak power of about 1.3 MVA [2].

The power supplies for BF and BD dipoles were developed and supplied directly to BNL by Danfysik A/S as a subcontractor of BINP. BINP produced the dipole power supply for magnetic measurements in ramp mode at BINP site [6]. All other power supplies were designed,

produced and delivered to BNL by BINP [7, 8]. Recently, all power supplies passed the acceptance tests at BNL both for DC mode and for 1-2Hz ramping mode. Figure 1 shows the example of BD power supply operation.

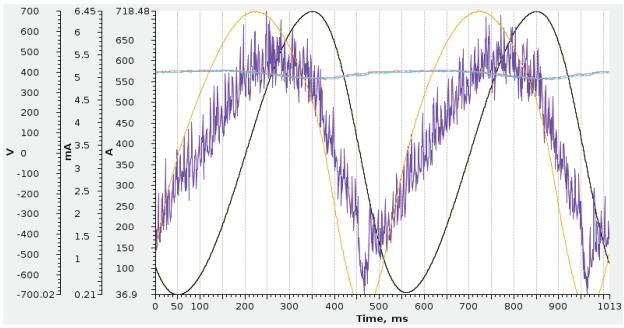

Figure 1: Current (black curve), voltage (yellow curve) and error signal (violet curve) plots for 2Hz cycles for BD power supply.

INJECTION AND EXTRACTION SYSTEM

For realization of the single injection and accumulation, four fast ferrite kickers and a pulse eddy-current type septum magnet are installed in the long straight section. The kicker and septum magnets are made out of vacuum.

The booster extraction system consists of four slow orbit bumpers, AC septum, DC septum and a kicker.

Injection and extraction AC septum and kicker are similar in design.

Table 3: Main Parameters of IES Magnets

Magnets	Q-ty	Magnetic length, m	Field T	Angle mrad	Pulse μs
Injection System for 200 MeV					
Kicker	4	0.207	0.055	17	0.3
Septum (AC)	1	0.75	0.11	125	100
Extraction System for 3 GeV					
Bump	4	0.17	0.46	7.8	1500
Kicker	1	0.83	0.073	6.1	0.3
Septum (AC)	1	0.6	0.8	48	150
Septum (DC)	1	1.2	0.89	106	-

After production, all the above-described elements were magnetically measured and heat tested with the pulsed power supplies developed by BINP.

To measure the pulsed magnets the special electronics has been developed [9]. These electronics provide the measurements of magnetic field with the accuracy of 5×10^{-5}.

The results of measurements are presented in the reports at this conference [10-13].

Currently, all of the elements are mounted at the booster ring and have successfully passed all tests.

VACUUM SYSTEM

At the moment, the whole vacuum system is assembled and pumped. Now the average obtained vacuum of the booster is better than 6×10^{-10} Torr. To check the ion pump efficiency, a test with air vent was done at the first assembled booster arc. The result of the experiment is shown in Figure 2.

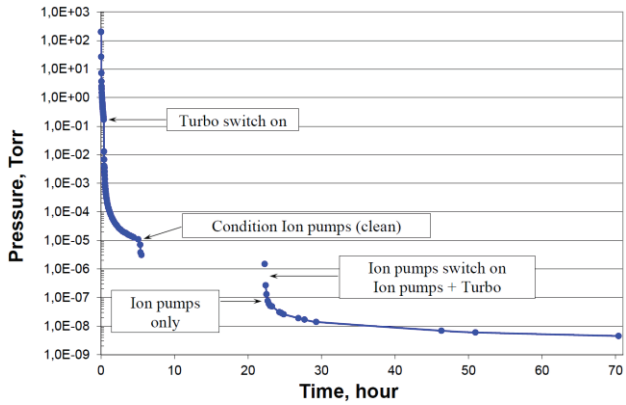

Figure 2: The pressure dynamics after air vent.

CONTROL SYSTEM

The booster control system [14, 15] is based on EPICS and provides continuous control of the all booster devices and diagnostics equipment during 1 or 2 Hz operation cycle of the booster. The use of the BNL developed Power Supply Controller (PSC) [16] allows us to precisely control ramping Power Supplies (PSs) with a time step of 0.1 ms and a relative time accuracy of about several nanoseconds with 20-bit DAC. At the same time PSC provides nine 16-bit ADCs for each DAC channel. Injection/Extraction pulsed PSs are also controlled with PSCs that allows a flexible driving of the energy storage charging process for a high stability of the pulsed output current. The Input/Output Controller running in the IBM server processes the measured 10k waveforms from each ADC channel and provides alarm signals in the case of unacceptable deviation of control and measured parameters.

An ability of the booster vacuum system is monitored by Allen Bradley PLC sets including check of Ion Pumps (IPs), Vacuum Gages (VGs) and valves status. These PLCs protect the vacuum chamber and produce interlock signals to inhibit operation of devices in the case of insufficient vacuum conditions. Vacuum devices such as IP and VG controllers are connected to the control system via serial interface.

The major part of the booster control software is developed in Control System Studio (CSS) [17] and Python. The PS engineering CSS screens allow us to manage and browse all controllable parameters of PSs [18]. The Ramp Manager (RM) python application provides a common interface to control all booster elements in a ramping mode. RM allows us to save/restore sets of ramping waveforms and to upload

ISBN 978-3-95450-122-9

waveforms to all booster devices including the RF system. Also a set of vacuum and interlock CSS screens is developed for the booster.

DIAGNOSTICS

For the Booster commissioning and operation all the equipment have been designed [19], manufactured and installed in the Booster ring and Injector Service Area. The Integrated Testing and the System Level Testing have been performed and some modification of the equipment has been done as a result of the testing [20].

A number of high-level applications has been developed using CSS and Python, including 1-st turn beam passing, Beam orbit monitor, BPM expert screen, Beam current monitor, DC Current Transformer and Fast Current Transformer expert screens, Booster tune monitor and Tune Measurement System expert screen, operator and expert screens for Beam flags and Synchrotron light monitors.

Thus, the beam diagnostic instrumentation is ready for the Booster commissioning.

SURVEY AND ALIGNMENT

At the first stage, the relative positions of fiducials on the magnetic elements and the position of fiducials relative to the magnetic axis of the element were defined. The magnetic axes of the elements were determined by the magnetic measurements using API Laser Tracker 3. The position determination accuracy of fiducials relative to the magnetic axis for dipoles was $\sigma = 0.065$ mm, for the quadrupole and sextupole was $\sigma = 0.035$ mm.

At the second stage, the magnetic elements were mounted on the girders and aligned according to the designed positions. The element positions were defined relative to the fiducials on the girders.

The magnetic element positions were determined using API Laser Tracker 3 relative to the designed positions with accuracy $\sigma = 0.085$ mm. Therefore, the positions of the magnetic elements on the girders relative to the calculated orbit was defined with accuracy

$$\sigma = \sqrt{0.065^2 + 0.085^2} = 0.107 mm .$$

On the basis of the performed measurements, the catalog of all fiducials of the girder assemblies in the booster coordinate frame has been created.

Now the booster ring is in process of the final alignment.

CONCLUSIONS

The NSLS-II booster project has gone through Integrating Testing stage. The booster is ready for commissioning.

ACKNOWLEDGMENT

We wish to thank BNL, BINP and DanFysik A/S teams involved in creation of the NSLS-II booster.

REFERENCES

[1] T.Shaftan et al., “NSLS-II Booster Design”, NSLS-II Tech. note 0061 (2009).
[2] S.Gurov et al., “Status of NSLS-II Booster”, PAC’11, New-York, April 2011, WEP201, p. 437 (2011);
[3] I.Okunev et al., “Magnetic Measurement of NSLS-II Booster Dipole Magnets with Combine Functions”, THPME032, these proceedings.
[4] S.Sinyatkin et al., “Magnetic Measurement Results of NSLS-II Booster Dipole Magnets”, THPME030, these proceedings.
[5] I.Okunev, et al., “Ramped Magnetic Measurement of NSLS-II Booster Dipoles”, THPME031, these proceedings.
[6] A.Erokhin et Al., “2Hz Ramping Mode Dipole Power Supply for Testing the NSLS-II Booster Dipole Magnets”, MOPWA025, these proceedings.
[7] D.Senkov et al., “Power System for Quadrupole Magnets of NSLS-II 3 GeV Booster”, MOPWA028, these proceedings.
[8] K.Yaminov et al., “Correcting Magnet Power Supplies for the NSLS-II Booster”, RUPAC’12, Saint-Petersburg, September 2012, WEPP027, p.500 (2012); http://www.JACoW.org.
[9] A.Pavlenko et al., “Electronics for Precise Measurement of Accelerator Pulsed Magnets”, THPEA033, these proceedings.
[10] A.Zhuravlev et al., “Pulsed Magnets for Injection and Extraction Sections of NSLS-II 3 GeV Booster”, THPME033, these proceedings.
[11] D.Shvedov et al., “Fast Magnetic Kickers for the NSLS-II Booster Synchrotron: Design and Test Results”, MOPWA026, these proceedings.
[12] A.Korepanov et al., “Pulse Power Supplies for Kicker Magnets of NSLS-II Booster Ring”, MOPWA027, these proceedings.
[13] D.Senkov et al., “Pulse Generators for Septums and Bumps of Injection and Extraction Systems of NSLS-II Booster”, MOPWA029, these proceedings.
[14] P.Cheblakov et al., "NSLS-II Booster Power Supplies Control", ICALEPCS’11, Grenoble, October 2011, WEPMS020, p.1018 (2011), http://www.JACoW.org.
[15] P.Cheblakov et al., "NSLS-II Booster Timing System", ICALEPCS’11, Grenoble, October 2011, WEPMS015, p.1003(2011), http://www.JACoW.org.
[16] Y.Tian et al., "NSLS-II Power Supply Controller", PAC’11, New-York, April 2011, TUP193, p.1187 (2011), http://www.JACoW.org.
[17] http://cs-studio.sourceforge.net/
[18] P.Cheblakov et al., “Software for Power Supplies Control of the NSLS-II Booster Synchrotron”, THPEA032, these proceedings.
[19] V.Smalyuk et al., “Beam Diagnostic for the NSLS-II Booster”, DIPAC’11, Hamburg, May 2011, MOPD01, p. 29 (2011), http://www.JACoW.org.
[20] O.Meshkov et al., “SLM and Flags for Booster of NSLS-II, MOPME064, these proceedings.